INTERNATIONAL JOURNAL OF ADVANCE RESEARCH, IDEAS AND INNOVATIONS IN TECHNOLOGY

ISSN: 2454-132X
Impact factor: 4.295
(Volume 4, Issue 2)
Available online at: www.ijariit.com

Grassberger procaccia algorithm for EEG channel selection

K. Navitha
navithavardhini@gmail.com
Padmasri Dr. B. V. Raju Institute of Technology, Medak, Telangana

Shaista Simmeen
Shaista07k@gmail.com
Padmasri Dr. B. V. Raju Institute of Technology, Medak, Telangana

K. Likhitha
likhithavarma55@gmail.com
Padmasri Dr. B. V. Raju Institute of Technology, Medak, Telangana

Jigar Patel
jigardotcom@gmail.com
Padmasri Dr. B. V. Raju Institute of Technology, Medak, Telangana

ABSTRACT

The multichannel nature of EEG a data poses a big challenge to the development of automatic EEG analysis and classification systems. Due to the "curse of dimensionality" problem, the analysis and classification of several channels may not lead to the desired performance. Accordingly, a number of algorithms have been proposed to identify small "static" subsets of channels that are capable of differentiating between samples of different classes. However, the identification of small subsets of relevant channels may not always be possible, where for certain applications the smaller the number of channels the less chance that sufficient information is provided. The propose in this project is a dynamic channel selection using Grassberger–Procaccia algorithm that identifies a channel (or a subset of channels) for each time segment of the signal that is relevant to the class of that particular time segment. To achieve this, we embraced the Grassberger–Procaccia algorithm methodology, and particularly the multiple classifier behaviour approach. Each EEG channel can be chosen to represent a certain unseen time segment of the signal based on the performance, or local accuracy, of its nearest neighbours in the set of training time segments. Results obtained using EEG data of a four-class alertness state classification problem reveal that the proposed approach is capable of achieving competitive performance compared to a traditional static channel selection based method. The algorithm also produced very encouraging results when a method developed by Grassberger Procaccia allows estimation of the dimensional complexity of the state-space attractor of a time series. Saturation of dimensional-complexity estimates with increasing values of embedding dimension is considered a strong indication that the time series is governed by deterministic chaos. The present investigation employed the Grassberger-Procaccia method to estimate EEG dimensional complexity in a multi-subject, factorial experiment.

Keywords: *GPFD (Grass Berger procaccia), BCI, EEG.*

1. INTRODUCTION

The Electroencephalography (EEG) signals have started to play increasingly important roles for many applications. These include the diagnosis of sleep disorders predicting epileptic seizures, building brain-computer interfaces detecting drivers' drowsiness, recognizing alertness state movement control and control of powered prosthetics for amputees and rehabilitation. It is well known that the utilization of multiple channels is essential for many of those applications. However, the usage of a large number of channels might have negative impact on the performance of automated analysis/classification systems, as this could increase the complexity of such systems. In this paper we consider the task of channel selection, i.e., selecting the most informative subset of channels that can achieve the best possible performance for a given EEG classification task. Most of the existing EEGchannel selection methods adopt a "static" selection approach, where a fixed subset of channels is identified and used to classify each and every time segment of the data. One of the advantages of the static approach is that the saving in computational effort is known a priori – it is simply the ratio of the number of selected channels to the total number of channels. Although static channel selection may enable the detection of redundant channels and the identification of channels that are highly influenced by noise, it is difficult to ascertain whether a subset of channels selected for one subject is also useful for other subjects, or to draw generalized conclusions about the most relevant channels for a given classification task across subjects.Also, since static methods cannot adapt to the specific data, valuable information may be lost or undetected. Dynamic channel selection, on the other hand, aims at using the results of the classification system to dynamically select which channel(s) to analyse for each time epoch. This provides the ability to adapt to changes in the EEG data by selecting the most relevant,

informative and noise free channels for each time segment of the data. However, the implementation of dynamic channel selection is far more challenging than its static counterpart.

2. DESIGN ANALYSIS

EEG Recording and Setting: EEG signals were recorded by a 24-channel electro-cap. The positions of the Ag/AgCl electrodes followed the international 10–20 system (see Figure 1). Electrode gel was applied to the electrodes to keep the impedance below 10 K Ohm. The ground channel was at the forehead, and the reference channels were at the mastoids (A1 and A2). The remaining 21 channels were all used to record EEG signals for analysis. Electrooculography (EOG) signals were recorded by the electrodes attached at the right side of the right eye and above of the left eye, respectively. Both EEG and EOG were amplified, band-pass filtered (0.5–100 Hz), and converted to digital signals with a sampling rate of 500 Hz using the NuAmp amplifier produced by NeuroScan Inc. The ocular artifacts were then removed from the EEG signals using the artifact removal software tool provided by the NeuroScan. The processed EEG signals were all stored in a personal computer for further offline analysis.

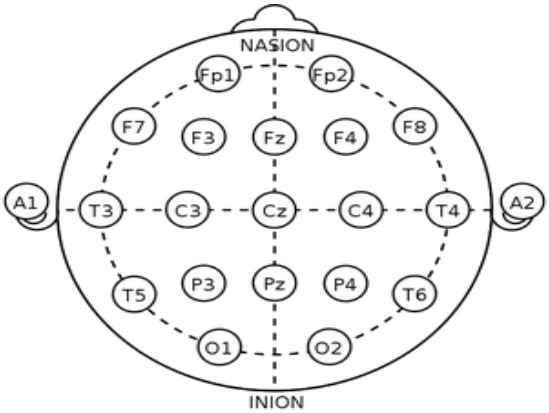

Fig. 1.Electrode placement

Table 1: List of Electrode Placement

Electrode	lobe
F	FRONTAL
T	TEMPORAL
C	CENTRAL
P	PARIETAL
O	OCCIPITAL

Preparation: The first four subjects sat in a wheelchair (Sub1 and Sub3) or normal armchair (Sub2 and Sub4) while facing a 20-inch computer screen. The Sub5 reclined in the bed. We projected the computer screen on the wall synchronously by a projector so that the instructions presented during the experiment could be clearly perceived by the Sub5. Three kinds of motor imagery tasks were designed in this study to test the classification accuracy of each motor imagery and no imagery (i.e., resting), including grasping an object by left hand (LH), grasping an object by right hand (RH), and stepping across a line in front of the subject with left foot (LF). All patients were provided with three pictures showing the three kinds of movements, respectively (Figure 2). They were asked to practice the imagination of the motions during the preparation stage (the stage of applying electro-gel to the 21electrodes). They were also informed of the motion decomposition in each movement in order to ensure the motor imagery contents across the subjects were consistent. For example, the movement of left foot stepping was decomposed to two motions: standing then stepping across the line with the left foot, as shown in Figure 2

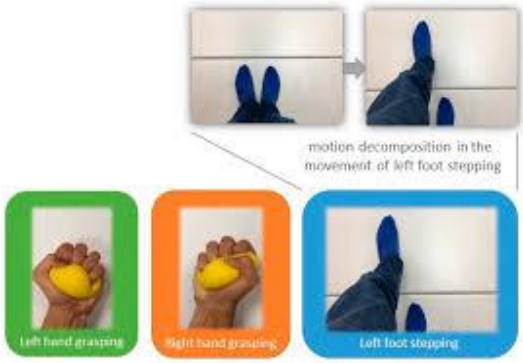

Fig. 2..Motor imagery tasks

Feature Extraction:

The GP algorithm estimates the correlation dimension (D2) or FD of an attractor in phase-space domain. Let x = [x(1), x(2), . . . , x(N)] denote the EEG signal of 3 s, where N is the length of the signal (N = 500 Hz × 3 s = 1500). The EEG signal can be reconstructed as a set of M-dimensional vectors as

$$y(i) = [x(i), x(i+\tau), x(i+2\tau), \ldots, x(i+(M-1)\tau)],\ i = 1, 2, \ldots, N-(M-1)\tau \quad \ldots (1)\ldots$$

where τ is the time delay and M is the embedding dimension. The time delay is a free parameter which needs to be determined experimentally.

$$C(r) = \frac{2}{N(N-1)} + \sum_{\substack{i,j=1 \\ i \neq j}}^{N-(M-1)\tau} H(r - |y(i) - y(j)|) \quad \ldots(2)\ldots$$

stands for the probability that the set of the distance between two different reconstructed vectors y(i) and y(j) (i.e., |y(i) − y(j)|, ∀i 6= j) fall into the cell of size r at a given embedding dimension M, where H is a Heaviside function defined as H(y) = 1 if y > 0; H(y) = 0 otherwise. The correlation dimension dc is given by

$$d_c(M) = \lim_{r \to 0} \left(\frac{\log C(r)}{\log(r)} \right)^n \quad \ldots(3)\ldots$$

The slope of log C(r) versus log r at a given M can be estimated over the region where log C(r) is approximately linear in log r by linear least-squares fitting. The slope of the line is the dc value at the given M. Moreover, the value of dc gradually increases with increase of M, and then achieves saturation. The saturation value is defined as the FD [29]. However, in numerical computation, the saturation value would not maintain at a constant, but varies slightly as the M

value further increases. Accordingly, the FD was determined based on the steps as follows,

Step 1. Initialize M = 2;
Step 2. M = M + 1;
Step 3. Calculate the dc value at the given M;
Step 4. Repeat step 2 and step 3 until |dc (M) − dc(M − 1)| < e; Step 5. FD = dc (M).

Where e is a positive number (we set e = 0.001). An excessively large value of epsilon could result in an M value for which the corresponding dc value has not yet saturated (e.g., M < 10). On the contrary, an excessively small value of epsilon could lead to the problem that no M value can be obtained. In this study, the e value was decided by trial and error. By using the setting of e = 0.001, the FDs of all EEG signals were obtained, and their M values were within the range of M > 10. Examples of the dc − M plots are shown in Figure 4, where each curve was calculated based on a 3-s EEG signal of a mental task. The four curves were based on the signals of resting, LH imagery, RH imagery, and LF imagery, respectively (all from patient Sub1 and recorded at F7). It can be observed from Figure 4 that the M values corresponding to the FDs (the dc values marked in black square) for the four different tasks are different (M = 23, 20, 21, 13 for the four tasks). According to our experiment, the GPFDs of all the EEG signals were found within the range of M = 10 to M = 30. Also, the M values associated with the GPFDs for different trials and different participants were not necessarily the same, depending the result by the aforementioned steps for the FD calculation.

Plots of dc against M for four 3-s EEG signals recorded under resting, left hand imagery, right hand imagery, and left foot imagery, respectively, and were all recorded at F7 from the patient participant Sub1. The correlation dimension □□ value marked in black in each curve is the FD estimated by the GP method. In this example, the □□ values for resting, left hand, right hand, and left foot conditions reached the plateau before ₹ = 30 (i.e., ₹ = 23, 20, 21, and 13, respectively). The FDs of the four signals are 4.2479, 3.4062, 3.9438, and 3.4577, respectively. The time delay was set as 50 for the four ca

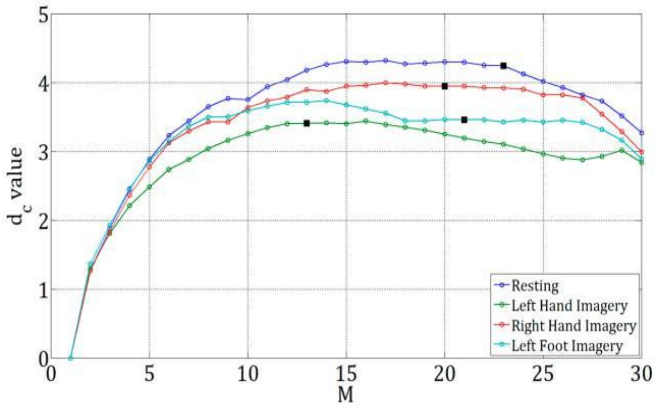

Fig. 3.Plots foe different subjects

3. RESULTS AND DISCUSSION

The average K-NN classification accuracies over the five subjects participants among different feature extraction methods, where the results shown in the three subplots are based on all 21 EEG channels (without channel selection), the top five channels, and the best channel, respectively. We used rank sum test to statistically examine the difference of classification accuracy between different feature extraction methods, because the one-sample test rejected the null hypothesis of normal distribution of the data ($p < 0.05$). Tables 2–4 list the top five channels and the corresponding RH-R, LH-R, and LF-R classification conditions. Different subbands in beta band may have different levels of beta rebound induced by a motor imagery . Therefore, we divided the mu and beta bands into five subbands, and computed the BP of the five subbands for the purpose of comparison.

S. No	Subject Name	Accuracy
1	Subject 1	60
2	Subject 2	62
3	Subject 3	65

Table 2: Accuracy of the Feature for Different

4. CONCLUSION

Motor imagery BCI has shown success on able-bodied individuals. Yet, there is still limited efficency in late-stage sub , which may be due to the fact that typical features, spectral information in the mu and beta bands, may not be as discriminative for sub . To deal with this problem, we have proposed in this paper a method by combining the GPFD feature channel selection strategy. Although the two separate methods have already been used in the BCI community, the use of GPFD and its combination with channel selection is novel for sub motor imagery classification. Our results have demonstrated that the proposed use of GPFD is superior to other features that have been used in previous studies involving subjects, and is able to achieve high accuracy (~90%) even when there is only one channel (the one selected by the proposed automatic subject-independent channel selection strategy). In summary, based on the results, it can be concluded that the contribution of the proposed method is three-fold. First, the use of the GPFD feature can provide motor imagery BCIs for subjects with higher accuracy. Second, the combination of the GPFD feature and channel selection strategy is able to automatically determine the best subject-dependent channel configuration from 30 EEG recording sites. Based on only a few selected channels, the GPFD can still maintain high average accuracy, which greatly improves the usability of the BCI for subjects discriminating channels for different subjects of motor imagery classification do not fall on the sensorimotor area. To our knowledge, this is a new finding in the EEG-based BCI community, and also supports the fMRI evidence that there is a spatial shift of function in the motor area in different subjects.

5. REFERENCES

[1] B. Platt and R. Gernot, ”The cholinergic system, EEG and sleep,” *Behav.Brain Res.*, vol. 221, no. 2, pp. 499-504, 2011.
[2] I. Koprinska, G. Pfurtscheller, and D. Flotzinger, ”Sleep Classification in Infants by Decision Tree-Based Neural Network,” *Artif. Intell. Med.*, vol.8, no. 4, pp. 387-401, 1996.
[3] P. Mirowski, D. Madhavan, Y. LeCun and R. Kuzniecky, ”Classificationof Patterns of EEG Synchronization for Seizure Prediction,” *Clin. Neuro.*,vol. 120, no. 11, 1927-1940, 2009.
[4] F. Siamac, J. Mehnert, J. Steinbrink, G. Curio, A. Villringer, K. R. Mller,and B. Blankertz, ”Enhanced performance by a hybrid NIRS-EEG braincomputer interface,” *Neuroimage*, vol. 59, no. 1, pp. 519-529, 2012.
[5] B. Gianluca, L. Astolfi, G. Vecchiato, D. Mattia, and F. Babiloni,”Measuring neurophysiological signals in aircraft

pilots and car driversfor the assessment of mental workload, fatigue and drowsiness," *Neurosci.Biobehav. Rev.*, ol. 44, pp. 58-75, 2014.
[6] L. Ning-Han, C. Y. Chiang, and H. M. Hsu, "Improving driver alertness through music selection using a mobile EEG to detect brainwaves," *Sensors*, vol. 13, no. 7, pp. 8199-8221, 2011.
[7] A. Al-Ani, M. Mesbah, B. Van Dun, and H. Dillon, "Fuzzy Logic-Based Automatic Alertness State Classification Using Multi-channel EEG Data," in Proc.*Int. Conf. Neural Inform. Process. (ICONIP)*, 2013, pp. 176-183,2013.
[8] J. Rafiee, M. Rafiee, F. Yavari, and M. Schoen, "Feature extraction offorearm EMG signals for prosthetics," *Expert Systems with Applications*,vol 38, pp. 4058-4067, 2011.
[9] A. Al-Timemy, R. Khushaba, G. Bugmann, and J. Escudero, "Improving
the Performance Against Force Variation of EMG Controlled Multifunctional
Upper-Limb Prostheses for Transradial Amputees," *IEEE TransNeural SystRehabilEng*, vol 23, 2015.
[10] B. Cesqui, P. Tropea, S. Micera and H.I. Krebs, "EMG-based patternrecognition approach in post stroke robot-aided rehabilitation: a feasibility study," *Journal of NeuroEngineering and Rehabilitation*, vol 10:75, 2013.
[11] M. Thulasidas, C. Guan and J. Wu, "Robust classification of EEG signalfor brain-computer interface," *IEEE Trans. Neural Syst. Rehabil. Eng.*,vol. 14, no. 1, pp. 24-29, 2006.
[12] A. Gonzalez, I. Nambu, H. Hokari and Y. Wada. Dynamic, "EEG channel selection using particle swarm optimization for the classification of auditory event-related potentials," *The Scient World J.*, pp. 1-12, 2014.
[13]Lotte, F.; Congedo, M.; Lécuyer, A.; Lamarche, F.; Arnaldi, B. A review of classification algorithms for EEG-based brain–computer interfaces. J. Neural Eng. 2007, 4, R1–R13.
[14]. Porro, C.A.; Francescato, M.P.; Cettolo, V.; Diamond, M.E.; Baraldi, P.; Zuiani, C.; Bazzocchi, M.; diPrampero, P.E. Primary motor and sensory cortex activation during motor performance and motor imagery: A functional magnetic resonance imaging study. J. Neurosci. 1996, 16, 7688–7698.
[15]. Khan, M.J.; Hong, M.J.; Hong, K.-S. Decoding of four movement directions using hybrid NIRS-EEG brain-computer interface. Front. Hum. Neurosci. 2014, 8, 1–10.
[16]. Naseer, N.; Hong, M.J.; Hong, K.-S. Online binary decision decoding using functional near-infrared spectroscopy for development of a brain-computer interface. Exp. Brain Res. 2014, 232, 555–564.

6. ACKNOWLEDGMENT

Authors are thankful to Cognitive sciences lab for utilizing the resources and also to the Department of ECE, BVRIT, Medak for the support and encouragement for writing this research article.

